Protein Science (1992), *1*, 259–270. Cambridge University Press. Printed in the USA.

Substrate polarization by residues in Δ^5-3-ketosteroid isomerase probed by site-directed mutagenesis and UV resonance Raman spectroscopy

JANINA C. AUSTIN,[1] ATHAN KULIOPULOS,[2,3] ALBERT S. MILDVAN,[2] AND THOMAS G. SPIRO[1]

[1] Department of Chemistry, Princeton University, Princeton, New Jersey 08544
[2] Department of Biological Chemistry, The Johns Hopkins University School of Medicine, Baltimore, Maryland 21205

(RECEIVED August 2, 1991; ACCEPTED September 18, 1991)

Abstract

Δ^5-3-Ketosteroid isomerase (KSI: EC 5.3.3.1) of *Pseudomonas testosteroni* catalyzes the isomerization of Δ^5-3-ketosteroids to Δ^4-3-ketosteroids by the stereospecific transfer of the steroid 4β-proton to the 6β-position, using Tyr-14 as a general acid and Asp-38 as a base. Ultraviolet resonance Raman (UVRR) spectra have been obtained for the catalytically active double mutant Y55F + Y88F, which retains Tyr-14 as the only tyrosine residue (referred to as the $Y14_0$ mutant), and the Y14F mutant, which has 50,000-fold lower activity. The UVRR results establish that binding of the product analog and competitive inhibitors 19-nortestosterone or 4-fluoro-19-nortestosterone to the $Y14_0$ mutant does not result in the formation of deprotonated Tyr-14. The UVRR spectra of the steroid inhibitors show large decreases in the vinyl and carbonyl stretching frequencies on binding to the $Y14_0$ enzyme but not on binding to the Y14F enzyme. These changes cannot be mimicked by protonation of the steroids. For 19-nortestosterone, the vinyl and carbonyl stretching frequencies shift down (with respect to the values in aqueous solution) by 18 and 27 cm^{-1}, respectively, on binding to $Y14_0$ KSI. It is proposed that the changes in the steroid resonance Raman spectrum arise from polarization of the enone moiety via the close proximity of the charged Asp-38 side chain to the vinyl group and the directional hydrogen bond between Tyr-14 and the 3-carbonyl oxygen of the steroid enone. The 230-nm-excited UVRR spectra do not, however, show changes that are characteristic of strong hydrogen bonding from the tyrosine hydrogen. It is proposed that this hydrogen bonding is compensated by a second hydrogen bond to the Tyr-14 oxygen from another protein residue.

UVRR spectra of the $Y14_0$ enzyme obtained using 200 nm excitation show enhancement of the amide II and S Raman bands. The secondary structure of KSI was estimated from the amide II and S intensities and was found to be low in α-helical structure. The α-helix content was estimated to be in the range of 0–25% (i.e., 10 ± 15%).

Keywords: Δ^5-3-ketosteroid isomerase; 19-nortestosterone; ultraviolet resonance Raman

The enzyme Δ^5-3-ketosteroid isomerase (KSI) from *Pseudomonas testosteroni* (EC 5.3.3.1) catalyzes the isomerization of Δ^5-3-ketosteroids to Δ^4-ketosteroids by a stereospecific and conservative transfer of the 4β-proton to the 6β-position (Schwab & Henderson, 1990; Xue et al., 1990; Kuliopulos et al., 1991). The catalytic reaction is generally thought to proceed via a dienolic intermediate (Fig. 1; Wang et al., 1963; Bantia & Pollack, 1986; Eames et al., 1990) by the concerted action of the enzyme residues Tyr-14 and Asp-38 (Kuliopulos et al., 1989; Xue et al., 1990). This intermediate proceeds to form product in either a concerted (Fig. 1) or stepwise process, the latter involving either a dienolate or carbonium ion intermediate. Many of the insights into the catalytic action of KSI have resulted from spectroscopic and structural studies of inhibitor–enzyme complexes (Kuliopulos et al., 1987b, 1989, 1991; Wang et al., 1963) and most recently, such studies have been enhanced by the use of site-directed mutants. In particular, the complexes of KSI and KSI mutants with the competitive inhibitor and product analog 19-nortestosterone have been

Reprint requests to: Thomas G. Spiro, Department of Chemistry, Princeton University, Princeton, New Jersey 08544.
[3] Present address: Department of Biological Chemistry and Molecular Pharmacology, Harvard Medical School, Boston, Massachusetts 02115.

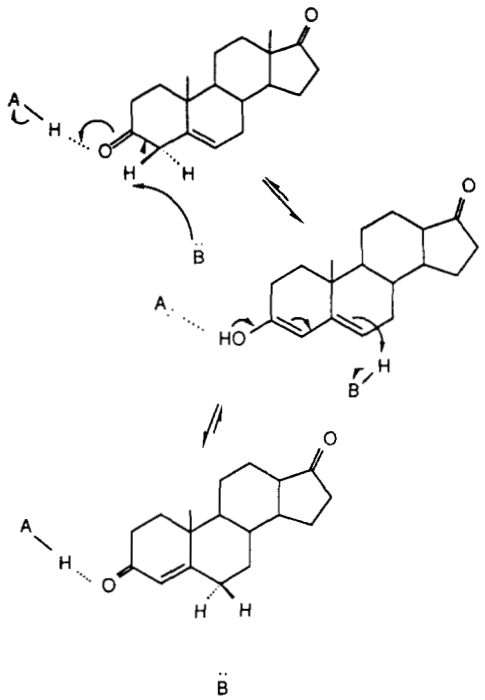

Fig. 1. Proposed reaction scheme for ketosteroid isomerase (Kuliopulos et al., 1991). The substrate enolization is concerted. The reketonization is shown as concerted for simplicity but may be stepwise, via a dienolate or a carbonium ion intermediate.

subject to intense study. The peculiar red-shift of the 19-nortestosterone absorption maximum on binding to KSI led to initial suggestions of protonation of the inhibitors' 3-carbonyl oxygen by the enzyme, or at least strong hydrogen bonding between an enzyme residue and the steroid carbonyl (Wang et al., 1963; Kuliopulos et al., 1989). The absorption spectral changes were found to be dependent on the presence of Tyr-14 in the enzyme active site, thus identifying this residue as the proton or hydrogen bond-donating residue. A recent ^{1}H NMR study of the complex of 19-nortestosterone bound to the catalytically active Y55F + Y88F double mutant of KSI presented evidence that Tyr-14 approached the anti lone pair of the 3-carbonyl oxygen of 19-nortestosterone to form a hydrogen bond (Kuliopulos et al., 1991).

Ultraviolet resonance Raman (UVRR) spectroscopy has recently emerged as a versatile probe of protein structure (Harada & Takeuchi, 1986; Hildebrandt et al., 1988; Su et al., 1989; Ames et al., 1990). Subtle changes in the hydrogen bonding of aromatic residues in proteins have been observed for hemoglobin as it switches from its R to T state (Su et al., 1989; Su, 1990). Protein secondary structure can be estimated from the intensities of two secondary structure-sensitive resonance Raman (RR) bands, amide II and amide S (Copeland & Spiro, 1987; Wang et al., 1991b). The present study uses UVRR spectroscopy to probe the structure of KSI, focusing on the interaction of Tyr-14 with its protein environment and on the interaction of Tyr-14 with the inhibitors 19-nortestosterone and 4-fluoro-19-nortestosterone (4FNT). KSI contains three tyrosine residues at positions 14, 55, and 88. The use of two specific mutants, the Y55F + Y88F double mutant (referred to here as the $Y14_0$ mutant) and the Y14F mutant, allows the distinction of spectral changes that are peculiar to the interaction of the inhibitors with Tyr-14. The tyrosine residues Tyr-55, Tyr-88, and Tyr-14 are found to experience noticeably different environments in the native enzyme, and the environment of Tyr-14 is found to change as the inhibitor 4FNT binds to the $Y14_0$ enzyme. UVRR spectra obtained using 200 nm excitation allow the KSI secondary structure to be described as being low in α-helical structure (ca. 10% α-helical).

The steroid inhibitors 19-nortestosterone and 4FNT can be selectively probed by UVRR spectroscopy, as they have strong absorptions in the region 250–260 nm. Dramatic changes in the UVRR spectra of the inhibitors are observed on binding to the $Y14_0$ enzyme. The close proximity of the carboxylate side chain of Asp-38 to the vinyl group of the steroid and the strong hydrogen bond between Tyr-14 and the steroid carbonyl provide a highly polar local environment of the steroid enone. The resulting polarized enone of the steroid gives rise to the large RR spectral changes observed as 19-nortestosterone and 4FNT bind to $Y14_0$ KSI. Conformational changes in the steroid A-ring cannot, in the present study, be ruled out, although it is concluded that large changes are unlikely.

Results and discussion

KSI polarizes the enone bonds of Δ^4-3-ketosteroids

Interaction of the enzyme with 19-nortestosterone and 4FNT

The absorption spectra of 19-nortestosterone and 4FNT are red-shifted on binding to $Y14_0$ KSI. The absorption maximum shifts from 248 to 256 nm for 19-nortestosterone and from 256 to ca. 265 nm for 4FNT bound to $Y14_0$ KSI. This red-shift can be mimicked if 19-nortestosterone is placed in acidic solution, which led to early suggestions of protonation or strong hydrogen bonding of the steroid as it binds to KSI. The absorption spectral shifts are not observed when 19-nortestosterone binds to the Y14F mutant of KSI (Kuliopulos et al., 1989), thus it has been suggested that the Tyr-14 residue protonates 19-nortestosterone as it binds to KSI. As mentioned in the preceding section, a recent ^{1}H NMR study (Kuliopulos et al., 1991) concluded that 19-nortestosterone is subject to hydrogen bonding, but not to protonation, on binding to $Y14_0$ KSI.

RR spectra were obtained for 19-nortestosterone bound to the $Y14_0$ and Y14F mutants, using 254 nm ex-

citation, where there is strong absorption from the bound inhibitor, but only weaker absorption from the enzyme and free inhibitor. The 254-nm-excited RR spectra of 19-nortestosterone bound to the $Y14_0$ and Y14F mutants of KSI are shown in Figure 2. Under the experimental conditions described, it can be assumed that the RR spectrum in Figure 2a arises entirely from enzyme-bound 19-nortestosterone. The RR spectrum in Figure 2b (Y14F + 19-nortestosterone) probably contains a significant (ca. 30%, see Materials and methods) contribution from free 19-nortestosterone; however, subtraction of the estimated free steroid contribution did not significantly alter the RR spectrum in Figure 2b. The spectrum of 19-nortestosterone in aqueous solution is shown for comparison in Figure 2c. For 4FNT, the excitation wavelength employed was 258 nm (although the absorption maximum is 265 nm), as longer wavelength excitation caused the RR spectra to be swamped by tyrosine fluorescence arising from uncomplexed enzyme. Steroid binding quenches tyrosine fluorescence dramatically (Wang et al., 1963), including the fluorescence from Tyr-14 (Kuliopulos et al., 1990). In addition, a small (two-fold) excess of 4FNT was added to the enzyme solutions to minimize the amount of uncomplexed enzyme, and thus fluorescence, from Tyr-14. The resulting RR spectra contained significant contributions from free 4FNT, as expected, but for presentation in Figure 2, the contribution to the RR spectrum of unbound inhibitor has been subtracted. The RR spectra (258 nm excitation) for 4FNT are presented in Figure 2, with the exception of the Y14F + 4FNT data. The RR spectrum of 4FNT bound to the Y14F enzyme could not be distinguished from the RR spectrum of the free steroid. The K_D of 4FNT could therefore not be determined. However, if it is assumed to be 30-fold greater than the K_D of 19-nortestosterone from the Y14F mutant (26.5 μM, Kuliopulos et al., 1989), as might be predicted from the 30-fold weaker binding of 4FNT to $Y14_0$ enzyme, then 15% of the steroid would be enzyme-bound in the RR experiment (see Materials and methods).

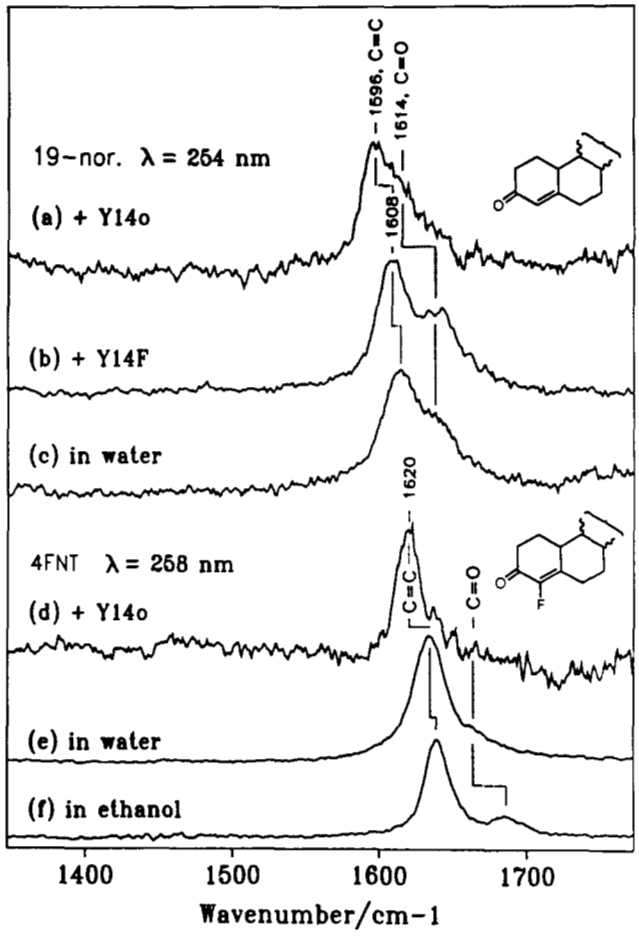

Fig. 2. The 254-nm-excited RR spectra of (**a**) $Y14_0$ KSI (subunit concentration = 185 μM) + 19-nortestosterone (200 μM), (**b**) Y14F KSI (subunit concentration = 180 μM) + 19-nortestosterone (200 μM), and (**c**) 19-nortestosterone in water. The 258-nm-excited RR spectra of (**d**) $Y14_0$ KSI (subunit concentration = 220 μM) + 4FNT (440 μM), the estimated contribution from free 4FNT has been subtracted; (**e**) 4FNT in water; and (**f**) 4FNT in ethanol (ethanol bands have been subtracted).

The RR spectrum of 19-nortestosterone in aqueous solution shows two bands at 1613.5 and 1641 cm^{-1}, which can be assigned as arising from predominantly C=C and C=O stretching vibrations, respectively. The positions of the Raman bands were determined by curve-fitting of two lorentzian bands to the spectrum. The 1641-cm^{-1} band retains its intensity in D_2O solution, thus it can be concluded that there is little contribution from the broad underlying water band (ca. 1640 cm^{-1}) to the RR spectra in Figure 2. The spectrum of 4FNT in water shows a strong RR band arising from the C=C stretching vibration at 1634 cm^{-1}, but only a weak carbonyl band at ca. 1661 cm^{-1}.

The RR spectra of both 19-nortestosterone and 4FNT are very perturbed on binding to the $Y14_0$ enzyme. For 19-nortestosterone, the vinyl RR band shifts from 1613.5 cm^{-1} to 1596 cm^{-1}, and the carbonyl band shifts from 1641 to ca. 1614 cm^{-1} on binding to $Y14_0$ KSI (Fig. 2a). The assignment of the two observed 19-nortestosterone vibrations on the $Y14_0$ enzyme as predominantly vinyl and carbonyl modes is made purely on the argument of the relative intensities (the vinyl mode is more intense in all the RR spectra). In the case of 4FNT, the vinyl mode shifts from 1634 to 1621 cm^{-1} on binding to $Y14_0$ KSI (see Fig. 2d,e). The weak carbonyl band cannot be assigned in the enzyme-bound 4FNT spectrum, due to overlap with the RR spectrum of unbound steroid. However, a lower limit for the shift of the carbonyl band can be set at around -20 cm^{-1}. The RR data are summarized in Table 1. The largest downshifts in the 19-nortestosterone carbonyl and vinyl (and 4FNT vinyl) RR bands are only observed when Tyr-14 is present in the enzyme active site. The RR spectrum of 19-nortestosterone bound to the Y14F enzyme (Fig. 2b) shows much smaller shifts in the vinyl band (6 cm^{-1}) and carbonyl band (ca. 0 cm^{-1}).

Table 1. *RR frequencies of 19-nortestosterone and 4FNT in solution and bound to KSI mutants*

System	$\nu_{C=C}/cm^{-1}$	$\nu_{C=O}/cm^{-1}$
19-nortestosterone in H_2O	1613.5[a]	1641[a]
19-nortestosterone + $Y14_0$	1596[a]	ca. 1614[a]
19-nortestosterone + Y14F	1608[a]	1641[a]
19-nortestosterone in 3.5 M H_2SO_4	1608	[b]
4FNT in H_2O	1634	1656
4FNT + $Y14_0$	1620	[b]

[a] Value determined after curve-fitting two lorentzian bands to the spectrum.
[b] Band not distinguishable.

A conformational change in 19-nortestosterone is unlikely

The spectral properties (absorption, IR, Raman) of enones are sensitive to their conformation (Gawronski, 1989). The downshifts in $\nu_{C=C}$ and $\nu_{C=O}$ upon binding might therefore reflect geometric distortions within 19-nortestosterone. Two types of conformational change have been shown to affect the absorption and IR spectra of enones, namely (1) variation of the torsional angle ω, O3-C3-C4-C5, and (2) twisting and pyramidilization of the vinyl group. The angle, ω, has been observed to be close to 180° in two crystal forms of 19-nortestosterone (Precigoux et al., 1975; Bhadbade & Venkatesan, 1984). Variation of ω from 180° is expected to produce blue-shifted absorption maxima and raised vibrational frequencies (House, 1983; Gawronski, 1989). Since this trend is opposite to the observed absorption and Raman spectral changes, it is reasonable to conclude that the torsional angle ω in 19-nortestosterone does not change as the molecule binds to KSI.

Deformation of the vinyl group has been reported to produce red-shifted absorption maxima (King and Morgan, 1960; Thiessen et al., 1971; House, 1983) and lowered vibrational frequencies (King and Morgan, 1960). However, C=C deformation would require force from the enzyme that would appear to be counterproductive to the enzyme mechanism. Because the proposed mechanism (Fig. 1) is favored by a planar conformation of the enone moeity, it is hard to see why (or how) the enzyme would act to produce such out-of-plane distortions. Such distortions therefore seem unlikely to explain the spectroscopic observations.

No evidence for dienolate formation from 19-nortestosterone

The formation of a dienolate species from a Δ^4-3-ketosteroid, such as 19-nortestosterone, can be seen as an intermediate in a stepwise reverse reaction of KSI (Fig. 1). The absorption maximum for $Y14_0$-bound 19-nortestosterone (λ_{max} = 260 nm) is close to the absorption maximum observed for the dienolate species generated in the reaction of Δ^5-androstene-3,17-dione with base (λ_{max} = 256 nm, Pollack et al., 1987). Although it is unlikely that a dienolate species is formed as 19-nortestosterone binds to KSI, it is worthwhile to characterize (by UVRR) the dienolate formed from Δ^5-androstene-3,17-dione so that the possibility can be dismissed. The rate constants for formation and decay of the dienolate in the solution reaction with base were recently determined as k_1 = 41 $M^{-1}\,s^{-1}$ and k_2 = 0.122 s^{-1} (Pollack et al., 1987). By mixing 0.25 M NaOH with Δ^5-androstene-3,17-dione in equal proportions, a 91% population of the dienolate can be achieved at t = 500 ms after mixing (see Materials and methods section for details of the mixing apparatus).

The RR spectrum of Δ^5-androstene-3,17-dione obtained using 258 nm excitation is shown in Figure 3a. The spectrum is weak, as the laser wavelength was chosen to selectively enhance the RR spectrum of the dienolate (the absorption maximum of Δ^5-androstene-3,17-dione in water is 238 nm). There is probably also a contribution of the RR spectrum of Δ^4-androstene-3,17-dione to the RR spectrum in Figure 3a, as a substrate Δ^5-3-ketosteroid is known to be contaminated by 5–6% of the product Δ^4-3-ketosteroid (the purity was checked by UV-visible absorption measurements both before and after reaction with KSI). The RR spectrum of the final

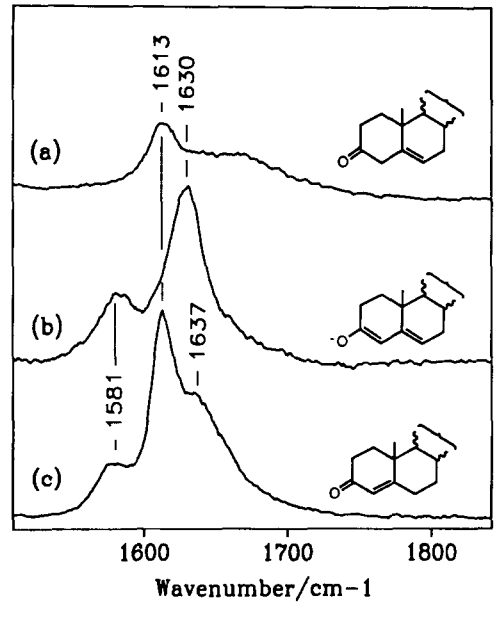

Fig. 3. The 258-nm-excited RR spectra of **(a)** Δ^5-androstene-3,17-dione in water, 0.2 mg/mL, 2% v/v methanol; **(b)** the dienolate species formed by mixing Δ^5-androstene-3,17-dione with 0.25 M NaOH; sum of spectra taken at t = 260 and 652 ms after mixing; and **(c)** the final product mixture of the reaction of Δ^5-androstene-3,17-dione with 0.25 M NaOH.

product mixture formed by mixing a 1:1 ratio of the Δ^5-androstene-3,17-dione solution with 0.25 M NaOH is shown in Figure 3c. The spectrum, with clear RR bands at 1613 and 1637 cm^{-1} is characteristic of the product Δ^4-androstene-3,17-dione—it is very similar to the spectrum of 19-nortestosterone in water. The RR spectrum of the dienolate (Fig. 3b) shows a strong new band at 1630 cm^{-1}, which is assigned to the symmetric stretch of the heteroannular trans-diene. This value is somewhat lower than the value of 1646 cm^{-1} observed for the symmetric stretch of 3,5-cholestadiene in water, which also contains a heteroannular trans-diene, reflecting increased π delocalization in the dienolate. The weaker band observed at 1581 cm^{-1} is also observed in the RR spectrum of the product mixture (Fig. 3c) and can probably be assigned as arising from a product of a side reaction. Because the 1630-cm^{-1} band is much higher than the bands of 19-nortestosterone bound to $Y14_0$, the RR data of the dienolate in solution strongly suggest that a dienolate species is not formed in the KSI active site when 19-nortestosterone is bound. The formation of a dienol species can be dismissed on the basis of the absorption spectra of the dienol formed from Δ^5-3-androstene-3,17-dione in solution (λ_{max} = 236 nm; Hawkinson et al., 1991) and bound to the D38N mutant of KSI (λ_{max} = 241 nm, Xue et al., 1991). The absorption maximum of the dienol is considerably blue-shifted with respect to the value observed for 19-nortestosterone bound to KSI (λ_{max} = 256 nm), thus making a dienol an extremely unlikely candidate for the species formed as 19-nortestosterone binds to KSI.

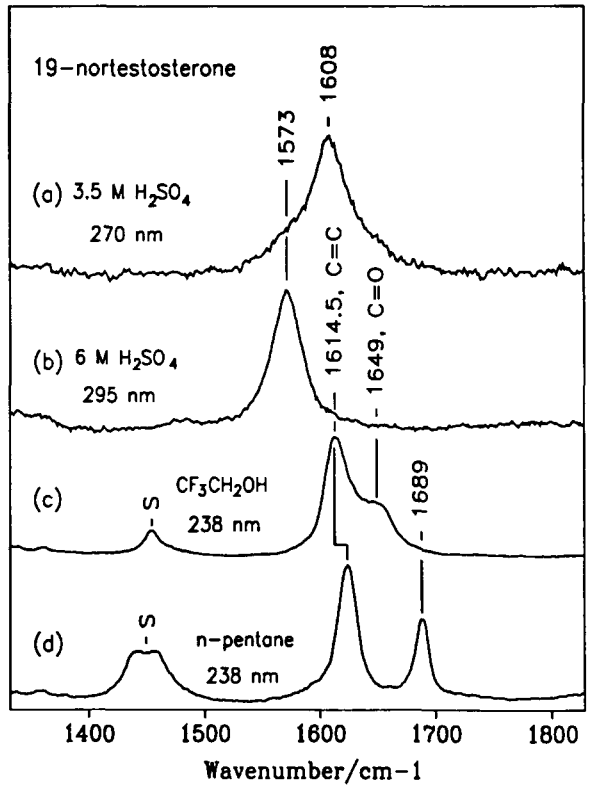

Fig. 4. (**a**) The 270-nm-excited RR spectrum of 19-nortestosterone in 3.5 M H_2SO_4. (**b**) The 295-nm-excited RR spectrum of 19-nortestosterone in 6 M H_2SO_4. (**c**) The 238-nm-excited RR spectrum of 19-nortestosterone in CF_3CH_2OH. (**d**) The 238-nm-excited RR spectrum of 19-nortestosterone in *n*-pentane. Peaks marked S are due to the solvent.

Is the steroid protonated?

To investigate the possibility of protonation of 19-nortestosterone on binding to the $Y14_0$ mutant of KSI, RR spectra of 19-nortestosterone in acidic solutions were obtained using 270- and 295-nm laser excitation, to selectively probe the different species that are formed in acidic media. It has been suggested that the species that is formed at higher pH (λ_{max} = 260 nm, 3.5 M H_2SO_4) is the protonated carbonyl species (I), whereas at lower pH (λ_{max} = 290 nm, 6 M H_2SO_4), a homoannular dienol species is formed (II) (Kuliopulos et al., 1989):

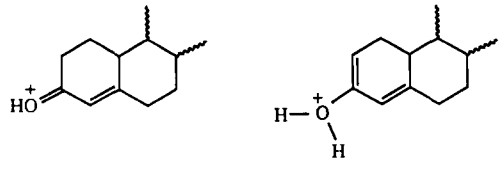

Species I Species II

The RR spectra of the two species are shown in Figure 4. The 290-nm-absorbing species has an RR band at 1573 cm^{-1} (Fig. 4b) that is assigned to the symmetric stretch of a substituted cis-diene—in agreement with the previous assignment of this solution species as the homoannular dienol. The value for the cis-diene symmetric stretching frequency in II (1573 cm^{-1}) is 32 cm^{-1} downshifted from the corresponding cis-diene stretching frequency observed for dehydrocholesterol in water (1605 cm^{-1}, data not shown). The 32-cm^{-1} downshift arises from the oxygen substituent at the 3-position in species II. The RR spectrum of the 260-nm-absorbing species of 19-nortestosterone (Fig. 4a) has a single RR band at 1608 cm^{-1}, which is assigned as the vinyl stretching mode of the simple protonated species (I). The absence of a carbonyl RR band in the spectrum in Figure 4a is probably due to weak enhancement of the protonated carbonyl, as has been reported for other protonated carbonyl species (Zalewski, 1989), and to the probable near overlap of the carbonyl and vinyl vibrations (see Fig. 5).

The RR spectra of protonated 19-nortestosterone (Fig. 4) do not show much similarity to the RR spectrum of the steroid bound to $Y14_0$ KSI. The enzyme-bound species has a significant RR contribution from both vinyl and carbonyl vibrations, and the vinyl frequency is more downshifted than the solution-protonated species that absorbs at the same wavelength. It is clear that pro-

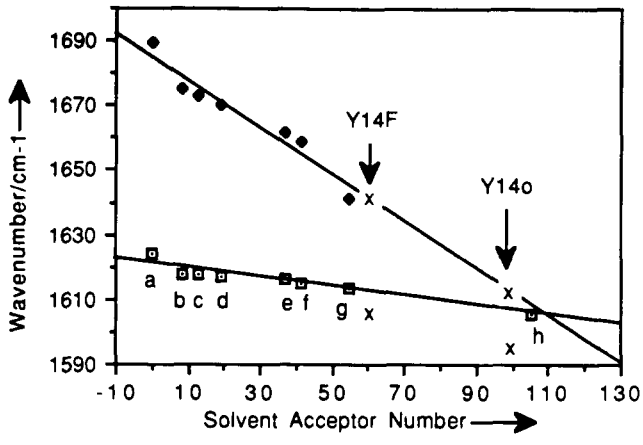

Fig. 5. Plot of $\nu_{C=C}$ and $\nu_{C=O}$ of 19-nortestosterone vs. solvent acceptor number (see also Table 2). a, *n*-pentane; b, benzene; c, acetone; d, acetonitrile; e, ethanol; f, methanol; g, water; h, trifluoroacetic acid. The wavenumber values for 19-nortestosterone bound to Y14F and $Y14_0$ KSI (crosses) are placed at AN values that best fit the C=O correlation (see text).

tonation of 19-nortestosterone (and 4FNT) is insufficient to explain the RR spectra of their complexes with KSI.

Polarity of the enzyme environment for 19-nortestosterone

In order to understand the unexpected result that binding to $Y14_0$ KSI produces a larger perturbation of the 19-nortestosterone RR frequencies than does protonation in aqueous H_2SO_4, we recorded RR spectra in a variety of solvents of different polarity (Table 2). Examples of the spectra in *n*-pentane and trifluoroethanol are shown in Figure 4 and reveal a marked sensitivity to the polarity. Figure 5 shows that linear correlations are obtained when $\nu_{C=C}$ and $\nu_{C=O}$ are plotted against solvent acceptor number (AN), a measure of the propensity of the solvent to accept electron pairs (as defined by the ^{31}P-NMR shift of a reference base ($(C_2H_5)_3PO$, Gutman, 1976). This parameter has previously been found to correlate well with amide carbonyl stretching frequencies (Grygon and Spiro, 1989; Wang et al., 1991a). The slope is about five times as large for $\nu_{C=O}$ as for $\nu_{C=C}$. This behavior is consistent with the view that solvents that are good electrophiles interact with the lone pairs on the O atom, polarizing and weakening the C=O bond; the C=C bond is also weakened because of its conjugation with C=O, but to a lesser extent. Thus, the C=O force constant decreases with increasing AN more rapidly than does the C=C force constant.

Table 2. *Raman frequencies of 19-nortestosterone in different solvents*

Solvent	AN[a]	$\nu_{C=C}$/cm^{-1}	$\nu_{C=O}$/cm^{-1}
Trifluoroacetic acid	105.3	1606	–[b]
Water	54.8	1613.5[c]	1641[c]
Trifluoroethanol	[d]	1614.5	1649
Methanol	41.3	1615	1659
Ethanol	37.1	1616	1662
Acetonitrile	18.9	1617	1670
Acetone	12.5	1618	1673
Benzene	8.2	1618	1675
n-Pentane	0	1624	1689

[a] AN, solvent acceptor number (Gutman, 1976).
[b] $\nu_{C=O}$ not distinguishable.
[c] Value determined after curve-fitting two lorentzian bands to the spectrum.
[d] AN value not available.

Because of the difference in slopes, the correlations between $\nu_{C=C}$, $\nu_{C=O}$, and AN in Figure 5 are expected to cross at sufficiently high AN. The extrapolation in Figure 5 shows the crossing point to occur at AN = 109, at which both $\nu_{C=O}$ and $\nu_{C=C}$ are predicted to be 1607 cm^{-1}. This is within 1 cm^{-1} of the frequencies observed for 19-nortestosterone in trifluoroacetic acid (AN = 105.3, Table 2) and in 3.5 M H_2SO_4 (Fig. 4). Thus, in addition to the expected loss in intensity of the $\nu_{C=O}$ Raman band upon carbonyl protonation, the observation of only one (albeit broad) band in the 3.5 M H_2SO_4 solution can be explained by the predicted near-coincidence of $\nu_{C=O}$ and $\nu_{C=C}$. If we use the $\nu_{C=O}$ frequency to place the $Y14_0$-19-nortestosterone complex on the plot in Figure 5 (crosses), we obtain a slightly lower effective AN than trifluoroacetic acid or 3.5 M H_2SO_4 (AN ~ 100), but the $\nu_{C=C}$ frequency falls significantly (12 cm^{-1}) below that predicted by the $\nu_{C=C}$/AN correlation. If the same procedure is applied to the Y14F-19-nortestosterone data, a negative deviation of $\nu_{C=C}$ is again seen, although it is smaller (5 cm^{-1}), and the effective AN is 60. This value of AN is larger than that of H_2O (AN = 55), a result that is quite surprising when one considers that the active site environment is decidedly hydrophobic, with Phe-82, Phe-86, Phe-100, and Val-74 all in close proximity to the steroid (Kuliopulos et al., 1987b), and with Phe replacing Tyr-14 at the carbonyl group. The Asp-38 side chain (which is presumably deprotonated) is, however, close to the vinyl group, placed to act as the base (B, Fig. 1) in the enzyme mechanism. This negative charge placed at the far end of the vinyl bond would polarize the enone moiety in the same direction as an electron acceptor molecule placed at the carbonyl oxygen. The polarizing effect of the Asp-38 side chain could account for the high effective AN observed in the Y14F enzyme, especially because of the hydrophobic environment, which prevents the charge from being screened by other polar interactions. It is reasonable that polarization via the vinyl end of the enone would produce a greater shift of the $\nu_{C=C}$ frequency than would polarization via the carbonyl end, thereby accounting for the negative deviation of $\nu_{C=C}$ from the AN correlation.

In the $Y14_0$-19-nortestosterone complex both Tyr-14

and Asp-38 are available to polarize the enone moiety. In addition, a recent NMR analysis (Kuliopulos et al., 1991) indicates that the hydrogen bond from Tyr-14 is directed along the trans lone pair of the carbonyl oxygen (angular), rather than through the Π electrons (linear). This has been shown to be the favored angle of approach for the hydrogen bonds in numerous crystal structures of cyclic enones (Murray-Rust & Glusker, 1984) and has also been shown to be the stronger type of hydrogen bond formed in solution (Laurence et al., 1985). All these factors conspire to strengthen the enone polarization and create an effective AN nearly as high as that corresponding to protonation of the carbonyl group. The $\nu_{C=C}$ frequency is characteristically lower than predicted by the AN correlation because of the effect of the negative charge in proximity to the vinyl group, an effect not modeled by varying the solvent.

Evidence for a compensating hydrogen bond to the Tyr-14 oxygen

Environment of Tyr-14 in the $Y14_0$ enzyme

The 230-nm-excited RR spectra of the $Y14_0$ and Y14F mutants of KSI are shown in Figure 6. The spectra are dominated by contributions from phenylalanine and tyrosine residues, as KSI contains no tryptophan. The differences in the mutant enzyme spectra largely reflect the different ratio of Tyr:Phe residues in each mutant (1:9 in $Y14_0$, 2:8 in Y14F). Detailed examination of the 1600-cm^{-1} region (see inset to Fig. 6) shows two prominent bands at 1606 and 1618 cm^{-1}, which are assigned to the phenylalanine ν_{8a} and tyrosine ν_{8a} vibrations, respectively (Harada & Takeuchi, 1986). A shoulder at 1596 cm^{-1} in the $Y14_0$ enzyme is assigned as the tyrosine ν_{8b} vibration. This shoulder is observed at 1599 cm^{-1} in the Y14F mutant, with ν_{8a} being at 1606 cm^{-1} for phenylalanine and at 1618 cm^{-1} for tyrosine. The ν_{8a} mode of phenylalanine is expected to remain unshifted in the $Y14_0$ and Y14F spectra, as it is generally assumed that phenylalanine residues are largely insensitive to environmental differences; relative intensities of RR bands can change, but frequency shifts have not been reported (Harada & Takeuchi, 1986; Hildebrandt et al., 1988; Su, 1990). The slight (less than 1 cm^{-1}) difference in the phenylalanine ν_{8a} band position in the Y14F and $Y14_0$ position probably reflects the intrinsic error in the measurement.

The shift in the tyrosine ν_{8b} band from 1599 cm^{-1} in the Y14F mutant to 1596 cm^{-1} in the $Y14_0$ mutant is indicative of a slight difference in the hydrogen-bonding environments of Tyr-14 and the other two tyrosine residues in KSI (Tyr-55 and Tyr-88). It has been demonstrated that there is a linear correlation between the Tyr-OH·····:A hydrogen-bond strength and the ν_{8b} position, the ν_{8b} band shifting to lower wavenumber with increased hydrogen-bond strength (Hildebrandt et al., 1988; Su, 1990). The correlation was recently reported as

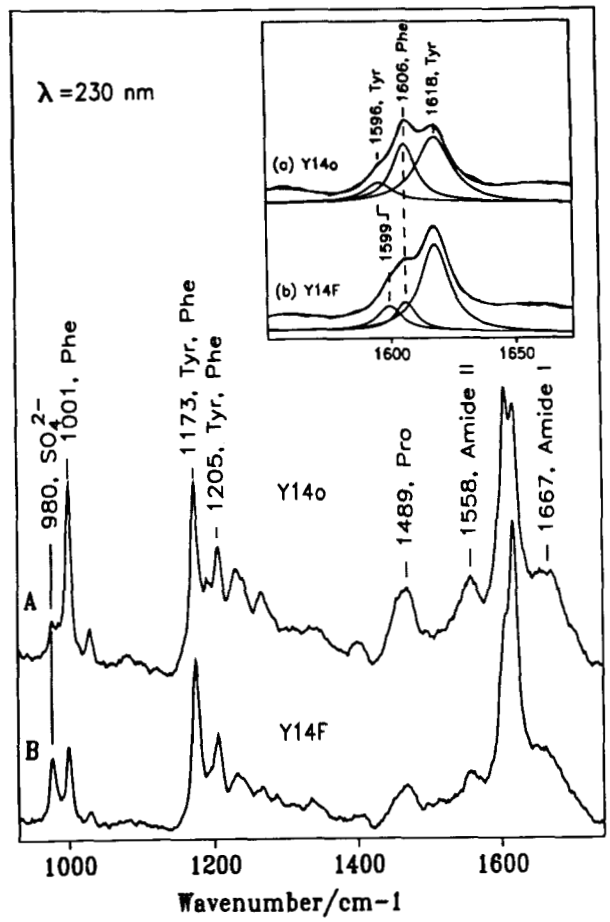

Fig. 6. The 230-nm-excited RR spectra of (**a**) $Y14_0$ KSI (subunit concentration = 220 μM) and (**b**) Y14F KSI (subunit concentration = 116 μM). Inset shows the $Y14_0$ and Y14F spectra (1600 cm^{-1} region only) with curve-fitted traces and fitted bands. The two broad bands fitted to the amide I and II bands are not shown for clarity.

$\nu_{8b} = 1598.0 - 0.8(-\Delta H)$, where 1598 refers to the frequency of the ν_{8b} band of *p*-cresol in cyclohexane, and ΔH is the hydrogen-bond enthalpy (Su, 1990). The position of the ν_{8b} band in the Y14F mutant (1599 cm^{-1}) is very close to that observed for *p*-cresol in a non-hydrogen-bonding environment (reported as 1598 cm^{-1} by Su [1990], but in the present study, the frequency was determined as 1600 cm^{-1}; this 2-cm^{-1} difference probably reflects a slight difference in the method of calibration). This observation suggests that Tyr-55 and Tyr-88 do not form measurable hydrogen bonds in the Y14F enzyme. In contrast, the apparent downshift of the tyrosine ν_{8b} mode to 1596 cm^{-1} for the $Y14_0$ mutant reflects a moderate (ca. 4 kcal/mol) hydrogen bond between Tyr-14 and an amino acid residue (or a water molecule) in the enzyme active site. It should be stressed that this estimate of hydrogen bonding to Tyr-14 is only approximate, given the inaccuracy in determining the position of an RR band that is strongly overlapped by other Raman bands. The tyrosine ν_{8b} frequency can be shifted by hydrogen bonding to

the phenolic oxygen atom, or by hydrogen bonding from the phenolic hydrogen. The two types of hydrogen bonding are reported to have opposite effects on the ν_{8b} frequency (Su, 1990). Thus, (1) a weak hydrogen bond between the Tyr-14 phenolic hydrogen and an acceptor group and (2) a stronger hydrogen bond offset by a hydrogen bond from a donor group to the Tyr-14 oxygen cannot be distinguished from the Tyr ν_{8b} frequency alone.

Environment and ionization state of Tyr-14 after inhibitor binding

The changes in the UVRR spectrum that accompany the deprotonation of tyrosine to form tyrosinate are substantial, with the ν_{8a} mode shifting from 1618 cm^{-1} to 1600 cm^{-1} and the ν_{8b} band shifting from 1600 to 1555 cm^{-1} (Asher et al., 1986; Hildebrandt et al., 1988). The $Y14_0$ mutant only contains one tyrosine; thus, deprotonation of Tyr-14 on binding 19-nortestosterone (or 4FNT) would be easily observed in the UVRR spectrum. The 230-nm-excited RR spectra of $Y14_0$ enzyme and of $Y14_0$ + 4FNT and the difference spectrum of (enzyme + steroid) − enzyme are compared in Figure 7. The difference spectrum obtained from the equivalent experiment using 19-nortestosterone is shown in Figure 7d. The difference spectra clearly show that tyrosinate is not formed when either 19-nortestosterone or 4FNT is bound to the active site of $Y14_0$ KSI. If tyrosinate were formed, the difference spectra would show a negative feature at ca. 1620 cm^{-1} and positive features at ca. 1600 and 1555 cm^{-1}.

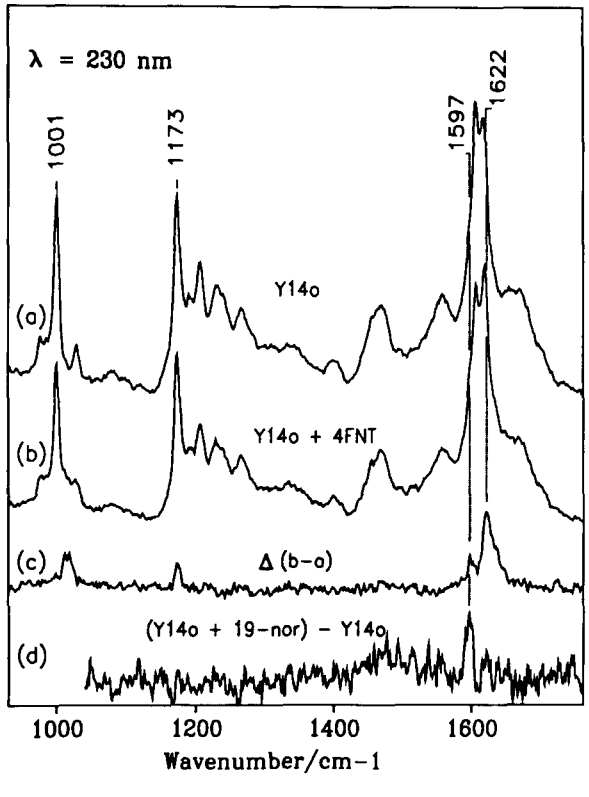

Fig. 7. The 230-nm-excited RR spectrum of **(a)** $Y14_0$ KSI, **(b)** $Y14_0$ KSI + 4FNT, **(c)** difference spectrum, b − a, and **(d)** equivalent difference spectrum of ($Y14_0$ + 19-nortestosterone) − $Y14_0$.

The largest features in the difference spectra at 1622 cm^{-1} (Fig. 7c) and 1596 cm^{-1} (Fig. 7d) can be assigned to the RR signals of the bound steroids, which are weak at 230 nm in relation to the aromatic residue bands but are detectable in the difference spectra. A small feature at ca. 1015 cm^{-1} in Figure 7c is assigned to the small amount of methanol added with the steroid. Due to the inferior quality of the data of 19-nortestosterone + $Y14_0$, and the severe overlap of the RR signals of the bound steroid and Tyr-14, it is impossible to discern if there is a significant perturbation of Tyr-14 on binding this inhibitor (Fig. 7d). In the case of 4FNT, however, there are small differences at 1597 cm^{-1} and 1172 cm^{-1} that can be assigned to changes in the tyrosine ν_{8b} and ν_{9a} modes. An intensification of the ν_{9a} mode and a 1-cm^{-1} upshift and intensification of the ν_{8b} mode are responsible for the differences in the enzyme and (enzyme + steroid) spectra, as judged by curve-fitting and self-deconvolution methods. These changes are consistent with a slight overall weakening of the Tyr-OH·····:A hydrogen bond. This observation is precisely opposite to the expected result, which would be a net increase in hydrogen bonding on inhibitor binding as the steroid 3-carbonyl oxygen hydrogen bonds to the Tyr-14 phenolic hydrogen. This unusual result can be rationalized if it is assumed that the moderate (ca. 4 kcal/mol) internal hydrogen bond of Tyr-14 to an enzyme acceptor is broken in the inhibitor:enzyme complex, and a slightly weaker (3 kcal/mol) hydrogen bond is formed between Tyr-14 and the steroid 3-carbonyl oxygen. However, this would contradict the conclusion drawn earlier from the RR data of the steroid, that a strong hydrogen bond is formed between Tyr-14 and and steroid 3-carbonyl. To explain the observed lack of change in the tyrosine ν_{8b} frequency and the large change in the steroids' RR spectrum, a more complex hydrogen-bonding scheme is proposed. A strong Tyr-14–steroid hydrogen bond is formed, replacing the existing hydrogen bond between the Tyr-14 hydrogen and an acceptor (probably water). Concomitant formation (or strengthening) of a hydrogen bond between a donor group and the Tyr-14 oxygen would offset the downshift in the ν_{8b} frequency expected for a strong steroid–Tyr-14 hydrogen bond. The latter scheme is shown in Figure 8.

Secondary structure of KSI

The UVRR spectrum of $Y14_0$ KSI obtained using 200 nm excitation is shown in Figure 9. A spectrum obtained of $Y14_0$ with 19-nortestosterone was essentially identical, within the signal-to-noise ratio of the data. The predominant modes in the spectrum arise from phenylalanine vibrations (at 1001, 1184 [shoulder], 1586 and 1606 cm^{-1})

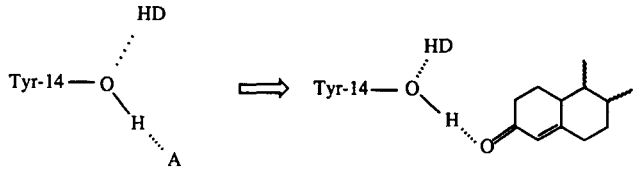

Fig. 8. Proposed hydrogen bonding in $Y14_0$ KSI, without and with 19-nortestosterone.

and from vibrations of the amide backbone (modes at 1237, 1389, 1555, and 1667 cm^{-1}). Tyrosine enhancement appears to be weak, as judged by the low intensity of the tyrosine Fermi doublet at 850 and 830 cm^{-1}; this is partly a consequence of the low number of tyrosine residues (one) in $Y14_0$ KSI relative to the number of phenylalanine residues but also reflects a real difference in the relative enhancement of the phenylalanine and tyrosine RR signals. The ratio of the area of the tyrosine Fermi doublet (850- and 830-cm^{-1} band areas combined) to the phenylalanine 1001-cm^{-1} band is 0.43. This value is not predicted by the ratio of the cross sections of these bands obtained at 200 nm in aqueous solution: the expected ratio is 2.3 (for a mixture 1 Tyr:9 Phe; Su et al., 1990). This discrepancy reflects the fact that these residues do not experience an aqueous environment but are buried in the protein. The resulting shifts in the Phe and Tyr $B_{a,b}$ absorptions due to the nonaqueous environment alter the relative RR enhancement of the Phe and Tyr signals; for example, the expected area ratio using 192 nm excitation is 0.17 (Su et al., 1990).

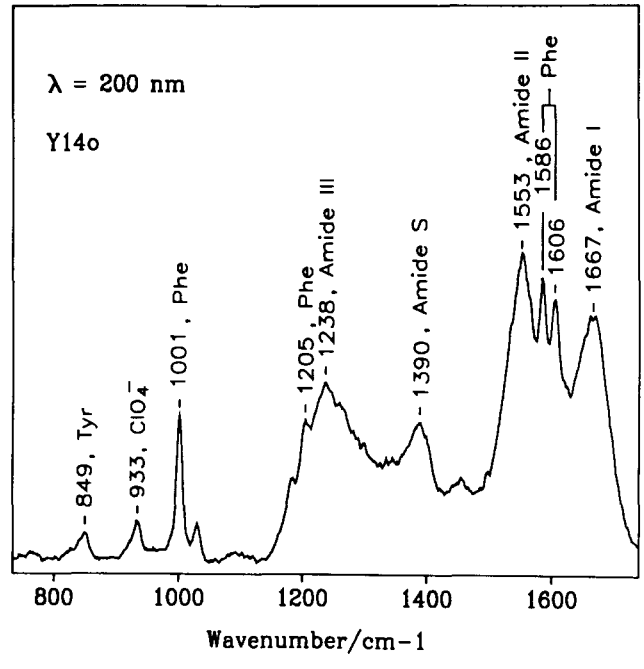

Fig. 9. The 200-nm-excited RR spectrum of $Y14_0$ KSI, 136 μM (subunit concentration) in pH 7 50 mM potassium phosphate buffer. Sodium perchlorate (0.2 M) was added as an internal intensity standard.

Curve-fitting of the entire spectrum with 19 lorentzian bands allows the relative heights and areas of the more overlapped amide S (1389 cm^{-1}) and amide II (1555 cm^{-1}) bands to be measured. Scaling of peak heights and areas relative to the perchlorate internal intensity standard yields a molar scattering ratio for the peptide group in the protein (the procedure has been described in detail by Wang et al., 1991b). Comparison of the KSI amide II and S molar scattering ratios with those obtained under similar experimental conditions for a selection of proteins of known structure (see Materials and methods) shows that there is a very low (ca. 10%) α-helical content in KSI. Although this value agrees with the helix content of 8% observed in the X-ray structure of KSI (Kuliopulos et al., 1987b), the relatively low perchlorate intensity (the protein concentration is higher than usually employed, 136 μM) and lack of correction for detector response makes the estimate prone to errors in the range of ±15% (i.e., helix content is between 0 and 25%). Further evidence in support of low α-helical content in KSI can be drawn from the positions of the amide III (1237 cm^{-1}) and amide I (1667 cm^{-1}) bands, which are at frequencies that are very indicative of a mixture of β-sheet and random structures (Tu, 1986).

Conclusions

The UVRR spectra of the product analogs 19-nortestosterone and 4FNT bound to KSI show strong depressions of the vinyl and carbonyl stretching frequencies of the critical enone moiety relative to the frequencies that would be expected for an enone in a nonpolar binding pocket. These frequency shifts are attributable to the combined effects of the Tyr-14 residue, which acts as a hydrogen-bond donor to the carbonyl oxygen, and of the Asp-38 residue, whose negatively charged carboxylate group is adjacent to the vinyl bond. These residues are the acid and base groups involved in the catalytic mechanism (Fig. 1). The UVRR data provide direct support for the mechanism shown in Figure 1 by revealing the strong polarization of the enone fragment, which is produced by the specific placement of Tyr-14 and Asp-38. This polarization produces a carbonyl frequency that is nearly as low as that produced by protonation in aqueous solution and a vinyl frequency that is even lower.

Despite this strong polarization, the Tyr-14 ν_{8b} frequency, a marker of the hydrogen-bond status, is essentially unperturbed by the steroid binding, whereas a substantial downshift is expected for strong hydrogen-bond donation (Su, 1990). This lack of shift can only be explained by a hydrogen-bond acceptor interaction of the Tyr-14 OH group with a donor residue, DH, which compensates the hydrogen-bond donation to the steroid car-

bonyl (Fig. 8). A compensating hydrogen-bond acceptor interaction suggests that a proton relay could be added to the enzyme mechanism in Figure 1, in which Tyr-14 is reprotonated by the donor DH as the Tyr-14 proton is transferred to the steroid carbonyl (Fig. 9). Alternatively, DH could stabilize the negatively charged tyrosinate formed in the intermediate of the KSI mechanism via a hydrogen-bonding interaction (Fig. 8). Intriguingly, deprotonation of a group with a pK_a of 9.7 ± 0.1 quenches Tyr-14 fluorescence by 50% (Kuliopulos et al., 1990); the pK_a of Tyr-14 exceeds 10.9 (Kuliopulos et al., 1991). Furthermore, the catalytic activity decreases as the pH is raised above 9.0, with an apparent pK_a ~9.5 (Wang et al., 1963; Weintraub et al., 1970). This suggests that a plausible candidate for the donor DH may be a lysine residue, which must be protonated to participate in the catalytic mechanism—additional evidence in support of the proposed proton relay.

Materials and methods

Protein preparation and assay

The procedures for overexpression and purification of the isomerase mutant enzymes to homogeneity were carried out as previously described (Kuliopulos et al., 1987a, 1989, 1991). Protein concentrations were calculated from the absorbance at 280 nm using typical absorption values for 1 mg/mL, pH 7, enzyme solutions of 0.226 for the Y14F mutant and 0.157 for the $Y14_0$ mutant in a 1-cm path-length cell (Kuliopulos et al., 1989, 1991). Specific activity measurements were made by monitoring the change in absorbance at 248 nm, at room temperature, of systems containing 50 mM Tris-HCl, pH 7.5, and 58.2 μM 5-androstene-3,17-dione, as described previously (Kuliopulos et al., 1989). Specific activity measurements made before and after UVRR experiments showed that there was a small decrease in activity during laser irradiation (30% per mW-hour of irradiation, at most 5–8% for a typical experiment). UV absorption measurements were made using a Hewlett Packard 8451A diode array spectrophotometer.

Resonance Raman spectroscopy

Enzyme samples for UVRR spectroscopy were made up to concentrations in the range of 130–200 μM in 50 mM potassium phosphate buffer, pH 7. Solutions of the steroids 19-nortestosterone and 4FNT in methanol were added to the enzyme solutions to give 1:1 ratios of enzyme:steroid (except in the 4FNT experiments undertaken with 258-nm excitation, see below) and final methanol concentrations of less than 3% v/v. As estimated from the K_D values (Kuliopulos et al., 1989, 1991), in the case of 19-nortestosterone, over 95% of the steroid is bound to the $Y14_0$ enzyme, and 70% is bound to the Y14F enzyme under the experimental conditions described. Under the conditions of a 1:1 ratio of steroid:enzyme, it follows that the enzyme occupancy is 95% for 19-nortestosterone bound to the $Y14_0$ enzyme and 70% for 19-nortestosterone bound to the Y14F enzyme. A K_D value for 4FNT binding to the $Y14_0$ enzyme was estimated from UV absorption difference spectra as ca. 30 μM (ca. 30-fold greater than with 19-nortestosterone). Thus, under the experimental conditions described, significantly less of the steroid is bound to the $Y14_0$ enzyme. For the experiments undertaken with 230-nm excitation, a 1:1 ratio of 4FNT:$Y14_0$ enzyme was used, resulting in 70% occupancy of the $Y14_0$ enzyme. For the experiments undertaken with 258 nm excitation, a 2:1 ratio of 4FNT:enzyme was employed, resulting in 90% occupancy of the $Y14_0$ enzyme, but only 45% bound steroid. A K_D value for 4FNT binding to the Y14F enzyme could not be obtained. If it is assumed that it is 30-fold greater than the value for 19-nortestosterone binding to the Y14F enzyme, a 2:1 ratio of 4FNT:Y14F would result in only 15% of the steroid being enzyme bound under the conditions described.

Samples were flowed in a guided wire-jet apparatus, in a recycling flow system using a peristaltic pump (total sample volume 3–4 mL) and were irradiated using approximate 135° backscattering geometry. The UV irradiation was focused at the sample, using average powers of 0.1–0.4 mW (at 200–300 Hz). The UV wavelengths in the range 290–200 nm were produced by frequency doubling or tripling the output of an excimer (Lambda Physik LPX130) pumped dye laser (Lambda Physik FL3002), as described by Wang et al. (1991a,b). The Raman-scattered light was collected using Cassegrain collection optics and dispersed using a Spex 1269 single monochromator equipped with a 3,600-groove/mm holographic grating (American Holographic). Raman scattering was detected using an image-intensified diode array (Princeton Instruments), cooled to −30 °C. Spectra were processed using Labcalc software (Galactic Industries Corp.). Calibration of the Raman spectra was performed using the known wavenumber values of Raman spectra of ethanol (protein spectra) or ethanol, acetone, and dimethylformamide (19-nortestosterone spectra). Spectra obtained using the same calibration were judged to be comparable to within 1 cm^{-1} (i.e., reported wavenumber differences between spectra are accurate to $\pm 0.5\ cm^{-1}$), although the absolute accuracy of the calibration is probably only $\pm 2\ cm^{-1}$.

The α-helical content of KSI was estimated from the 200-nm RR spectrum of 136 μM KSI in pH 7 phosphate buffer (with 0.2 M $NaClO_4$ as an internal intensity standard) using the following procedure. Proteins of known structure were dissolved in 50 mM potassium phosphate buffer, pH 7, to final concentrations of 1 mg/mL, with 0.15 M $NaClO_4$ as an internal intensity standard. The proteins used (Sigma) were concanavalin A, ribonuclease, trypsin, hemoglobin, myoglobin, cytochrome c (equine),

and lysozyme. The 200-nm RR spectra of all the samples (including KSI) were processed to give values of the molar scattering intensity ratio, R, as described by Wang et al. (1991b). The R values obtained for the amide S and II Raman bands of the proteins of known structure were found to be consistently larger than the corresponding R values obtained by Wang et al. (1991b). The R values were, on average, 1.8-fold (amide S) and 2.0-fold (amide II) larger (the reason for the discrepancy is not clear). The R values obtained for the KSI amide S and II bands were divided by the factors 1.8 and 2.0, respectively. These adjusted R values for KSI were used (with the secondary structure correlation of Wang et al.) to determine the α-helix content of the protein. A new correlation was not determined, as it was judged that the fewer number of data points obtained for the proteins of known structure would make the measurement more prone to error.

Formation of the dienolate

The dienolate species was generated by the reaction of Δ^5-androstene-3,17-dione with sodium hydroxide (Pollack et al., 1987), using a continuous flow apparatus. A solution of Δ^5-androstene-3,17-dione (0.2 mg/mL) in water (2% v/v methanol) was mixed with a solution of 0.25 M NaOH. Δ^5-Androstene-3,17-dione was a generous gift from Dr. Paul Talalay. Solutions were filtered (Millipore) and degassed prior to mixing and placed in two 50-mL syringes connected to a mixing chamber (Wiskind Model 1155, Update Instruments). Flow rates of 1.84 and 4.6 mL/min were produced using a syringe pump (Harvard Instruments). The mixed solution was flowed in a quartz capillary tube (0.5 mm internal diameter), where the laser excitation was focused at approximately 10 cm from the mixing point. The age of the sample at the laser spot is calculated from the flow rate to be approximately 260 and 652 ms for the two flow rates employed (1.84 and 4.6 mL/min). The mixing efficiency was tested by monitoring the reaction of HSO_4^- with OH^- (as described by Simpson et al., 1986); the diffusion-controlled reaction was found to be essentially complete under the range of flow rates used for the experiment.

Acknowledgments

We are grateful to Paul Talalay for helpful advice and materials throughout the course of this work. These studies were supported by grants GM25158 (T.G.S.), DK28616 (A.S.M.), and DK07422 (to Paul Talalay), all from the NIH.

References

Ames, J.B., Bolton, S.R., Netto, M.M., & Mathies, R.A. (1990). Ultraviolet resonance Raman spectroscopy of bacteriorhodopsin: Evidence against tyrosinate in the photocycle. *J. Am. Chem. Soc. 112*, 9007–9009.

Asher, S.A., Ludwig, M., & Johnson, C.R. (1986). UV resonance Raman excitation profiles of the aromatic amino acids. *J. Am. Chem. Soc. 108*, 3186–3197.

Bantia, S. & Pollack, R.M. (1986). Evidence for an enol intermediate in the 3-oxo-Δ^5-steroid isomerase catalysed isomerization of Δ^5-ketones. *J. Am. Chem. Soc. 108*, 3145–3146.

Bhadbhade, M.M. & Venkatesan, K. (1984). Conformational flexibility in androgenic steroids: The structure of a new form of (+)-17b-hydroxy-19-nor-4-androstene-3-one (19-nortestosterone), $C_{18}H_{26}O_2$. *Acta Crystallogr. C40*, 1905–1908.

Copeland, R. & Spiro, T.G. (1987). Secondary structure determination in proteins from deep (192–223 nm) ultraviolet Raman spectroscopy. *Biochemistry 26*, 2134–2139.

Eames, T.C.M., Hawkinson, D.C., & Pollack, R.M. (1990). Direct determination of the partitioning of an enzyme-bound intermediate. *J. Am. Chem. Soc. 112*, 1996–1998.

Gawronski, J. (1989). Spectral properties of enones. In *The Chemistry of Enones*, Part 1 (Patai, S. & Rappoport, Z., Eds.), pp. 55–105. Wiley, New York.

Grygon, C.A. & Spiro, T.G. (1989). Ultraviolet resonance Raman spectroscopy of distamycin complexes with poly(dA)-poly(dT) and poly (dA-dT): Role of H-bonding. *Biochemistry 28*, 4397–4402.

Gutman, V. (1976). Solvent effects on the reactivities of organometallic compounds. *Coord. Chem. Rev. 18*, 225–255.

Harada, I. & Takeuchi, H. (1986). Raman and ultraviolet resonance Raman spectra of proteins and related compounds advances. In *Infrared and Raman Spectroscopy: Spectroscopy of Biological Molecules*, Vol. 13 (Clark, R.J.H. & Hester, R.E., Eds.), pp. 113–175. Wiley, New York.

Hawkinson, D.C., Eames, T.C.M., & Pollack, R.M. (1991). Kinetic competence of an externally generated dienol intermediate with steroid isomerase. *Biochemistry 30*, 6956–6964.

Hildebrandt, P.G., Copeland, R.A., Spiro, T.G., Otlewski, J., Laskowski, M., & Prendergast, F.G. (1988). Tyrosine hydrogen bonding and environmental effects in proteins probed by ultraviolet resonance Raman spectroscopy. *Biochemistry 27*, 5426–5433.

House, H.O. (1983). Enones with distorted double bonds. In *Stereochemistry and Reactivity of Systems Containing II Electrons* (Watson, W.H., Ed.), pp. 279–317. Verlag-Chemie Int., Deerfield Beach.

King, F.E. & Morgan, J.W.W. (1960). The chemistry of extractives from hardwoods. Part XXX. The constitution of katonic acid, a triterpene from *Sandoricum indicum*. *J. Chem. Soc.*, 4738–4747.

Kuliopulos, A., Mildvan, A.S., Shortle, D., & Talalay, P. (1989). Kinetic and ultraviolet spectroscopic studies of active site mutants of Δ^5-3-ketosteroid isomerase. *Biochemistry 28*, 149–159.

Kuliopulos, A., Mullen, G.P., Xue, L., & Mildvan, A.S. (1991). Stereochemistry of the concerted enolization catalysed by Δ^5-3-ketosteroid isomerase. *Biochemistry 30*, 3169–3178.

Kuliopulos, A., Shortle, D., & Talalay, P. (1987a). Isolation and sequencing of the gene encoding Δ^5-3-ketosteroid isomerase of *Pseudomonas testosteroni:* Overexpression of the protein. *Proc. Natl. Acad. Sci. USA 84*, 8893–8897.

Kuliopulos, A., Talalay, P., & Mildvan, A.S. (1990). Fluorescence and NMR properties of the sole tyrosine (Tyr-14) in a double mutant of Δ^5-3-ketosteroid isomerase (KSI). *Biochemistry 29*, 2197 (Abstr. 99).

Kuliopulos, A., Westbrook, E.M., Talalay, P., & Mildvan, A.S. (1987b). Positioning of a spin-labeled substrate analogue into the structure of Δ^5-3-ketosteroid isomerase by combined kinetic, magnetic resonance, and X-ray diffraction methods. *Biochemistry 26*, 3927–3937.

Laurence, C., Berthelot, M., & Helbert, M. (1985). Stereochimie de la liason hydrogene sur le groupe carbonyle. *Spectrochim. Acta 41A*, 883–892.

Murray-Rust, P. & Glusker, J.P. (1984). Directional hydrogen bonding to sp^2- and sp^3-hybridized oxygen atoms and its relevance to ligand–macromolecule interactions. *J. Am. Chem. Soc. 106*, 1018–1025.

Pollack, R.M., Mack, J.P.G., & Eldin, S. (1987). Direct observation of a dienolate intermediate in the base-catalyzed isomerization of 5-androstene-3,17-dione to 4-androstene-3,17-dione. *J. Am. Chem. Soc. 109*, 5048–5050.

Precigoux, P.G., Busetta, B., Corseille, C., & Hospital, M. (1975). Structure cristalline et moleculaire de la nor-19 testosterone. *Acta Crystallogr. B31*, 1527–1532.

Schwab, J.M. & Henderson, B.S. (1990). Enzyme-catalyzed allylic rearrangements. *Chem. Rev. 90*, 1203–1245.

Simpson, S.F., Kincaid, J.R., & Holler, F.J. (1986). Development of a microdroplet mixing technique for the study of rapid reactions by Raman spectroscopy. *Anal. Chem. 58*, 3136–3166.

Su, C. (1990). Hemoglobin structure and dynamics studies by ultraviolet resonance Raman spectroscopy. Ph.D. Thesis, Princeton University, Princeton, New Jersey.

Su, C., Park, Y.D., Liu, G.-Y., & Spiro, T.G. (1989). Hemoglobin quaternary structure change monitored directly by transient UV resonance Raman spectroscopy. *J. Am. Chem. Soc. 111*, 3457–3459.

Su, C., Wang, Y., & Spiro, T.G. (1990). Saturation effects on ultraviolet resonance Raman intensities: Excimer/YAG laser comparison and aromatic amino acid cross sections. *J. Raman Spectrosc. 21*, 435–440.

Thiessen, W.E., Levy, H.A., Dauben, W.G., Beasley, G.H., & Cox, D.A. (1971). A highly twisted carbon-carbon double bond. *J. Am. Chem. Soc. 93*, 4312–4314.

Tu, A. (1986). Peptide backbone conformation and microenvironment of protein side chains: In *Advances in Infrared and Raman Spectroscopy: Spectroscopy of Biological Molecules*, Vol. 13 (Clark, R.J.H. & Hester, R.E., Eds.), pp. 47–112. Wiley, New York.

Wang, S.F., Kawahara, F.S., & Talalay, P. (1963). The mechanism of the Δ^5-3-ketosteroid isomerase reaction: Absorption and fluorescence spectra of enzyme-steroid complexes. *J. Biol. Chem. 238*, 576–585.

Wang, Y., Purrello, R., Georgiou, S., & Spiro, T.G. (1991a). UVRR spectroscopy of the peptide bond II: Carbonyl H-bond effects on the ground and excited state structures of N-methylacetamide. *J. Am. Chem. Soc. 113*, 6368–6377.

Wang, T., Purrello, R., Jordan, T., & Spiro, T.G. (1991b). UVRR spectroscopy of the peptide bond I: Amide S, a non-helical structure marker is a $C_\alpha H$ bending mode. *J. Am. Chem. Soc. 113*, 6359–6368.

Weintraub, H., Alfsen, A., & Baulieu, E.-E. (1970). Etude de la $\Delta_{5\to4}$ 3-oxosteroide isomerase: Caracteristiques des groupes impliques dans le transfert de protons. *Eur. J. Biochem. 12*, 217–221.

Xue, L., Kuliopulos, A., Mildvan, A.S., & Talalay, P. (1991). Catalytic mechanism of an active-site mutant (D38N) of Δ^5-3-ketosteroid isomerase: Direct spectroscopic evidence for dienol intermediates. *Biochemistry 30*, 4991–4997.

Xue, L., Talalay, P., & Mildvan, A.S. (1990). Studies of the mechanism of the Δ^5-3-ketosteroid isomerase reaction by substrate, solvent, and combined kinetic deuterium isotope effects of wild-type and mutant enzymes. *Biochemistry 29*, 7491–7500.

Zalewski, R.I. (1989). Acid–base behaviour of enones. In *The Chemistry of Enones*, Part 1 (Patai, S. & Rappoport, Z., Eds.), pp. 328–329. Wiley, New York.